MCST Internal Memo

Date: December 11, 2020

From: Tiejun Chang, Ashish Shrestha, Carlos Perez Diaz, Aisheng Wu, Yonghong Li, Na Chen and Truman Wilson

To: MODIS Science Team members Subject: Proposed calibration improvements for the MODIS thermal emissive bands in Collection 7 Level 1B processing

Memo #: M1163

---

1. INTRODUCTION

1.1 MODIS TEBs Collection 6.1

The current MODIS Collection 6.1 (C6.1) look-up table (LUT) on-orbit update algorithms for the Terra and Aqua MODIS TEBs are summarized in Table 1.1-1 [1]. The band 21 b_1 linear coefficient (not described in Table 1.1-1) is derived using the on-board blackbody (BB) cooldown (CD) data - with the offset and non-linear calibration terms constrained to zero in the fitting algorithm. The Terra MODIS photoconductive (PC) longwave infrared (LWIR) TEBs crosstalk coefficients were derived using lunar observation analyses from the mission beginning. Moreover, an electronic crosstalk correction is applied to Terra MODIS photovoltaic (PV) LWIR bands 27-30 during calibration and Earth view (EV) retrievals. The Aqua C6.1 MODIS TEBs use the pre-launch a_0 and pre-launch adjusted a_2 calibration coefficients for all bands – except for bands 31 and 32 (a_0 is equal to zero and a_2 is derived using the CD data) [2]. In a general sense, brightness temperature (BT) difference analyses between the current LUT and newly derived a_0 and a_2 calibration coefficients are performed to verify if a forward LUT update of the calibration algorithm coefficients is necessary. If the update criteria are exceeded, a LUT update is issued to meet the radiometric accuracy requirements of the L1B data in forward production.

Additional LUTs are updated on a need basis for the MODIS C6.1 TEBs. These include those used to calculate the time-dependent uncertainty index (UI) - updated after every calibration coefficients LUT update, the time-dependent quality assessment (QA) LUT, and the Aqua default b1 LUT.

Table 1.1-1 Terra and Aqua MODIS C6.1 TEBs calibration algorithms.

(PL: pre-launch; CD: cooldown)

Band	Aqua	Terra	
	Calibration algorithm	Calibration algorithm	Cross-talk correction
20	PL a_0 PL adjusted CD a_2	$a_{0\_ms1} = 0$ $a_{0\_ms2} = a_{0\_ms2}^{\text{free-fit}} - a_{0\_ms1}^{\text{free-fit}}$ CD a_2	
22			
23			
24			
25			
27			PV LWIR electronic cross-talk
28			
29			
30			
31	a_0=0, CD a_2	$a_0 = 0$ CD a_2	
32			PC LWIR optical cross-talk
33	a_0=0 PL adjusted CD a_2		
34			
35			
36			

1.2 Recommendations for C7 algorithm improvements

Several calibration algorithm improvements were discussed, tested, validated, and are hereby proposed by MCST in preparation for C7. These are listed below, and the recommended MODIS C7 LUT update algorithms for the Terra and Aqua MODIS TEBs are summarized in Table 1.2-1. Detailed algorithm descriptions for Terra and Aqua MODIS are presented in Sections 3 and 4, respectively.

A. Terra MODIS TEBs

(1) Midwave infrared (MWIR) bands crosstalk correction for selected detectors

(2) Early mission PC bands a_0 correction to reduce mirror side difference

(3) Bands 20 and 29 a_0 correction and a_2 re-processing to decrease cold scene bias

(4) Use of fixed a0 and a2 for B30 to improve its calibration stability for Band 30

B. Aqua MODIS TEBs

(1) MWIR and LWIR bands crosstalk correction for selected detectors

(2) Mission-long a_0 correction and a_2 update using BB CD data to reduce mirror side difference

Table 1.2-1 Terra and Aqua MODIS C7 TEBs calibration algorithms recommendations.

(MS: mirror side; PL: pre-launch; CD: cold-down)

<table>
<tr><th rowspan="2">Band</th><th colspan="2">Aqua</th><th colspan="2">Terra</th></tr>
<tr><th>Calibration algorithm</th><th>Cross-talk correction</th><th>Calibration algorithm</th><th>Cross-talk correction</th></tr>
<tr><td>20</td><td rowspan="10">PL a_0 with MS correction

CD a_2</td><td rowspan="10">Electronic cross-talk corrections for selected detectors</td><td>Corrected a_0; CD a_2</td><td rowspan="2">Electronic cross-talk corrections for selected detectors</td></tr>
<tr><td>22</td><td rowspan="5">$a_{0\_ms1} = 0$
$a_{0\_ms2} = a_{0\_ms2}^{\text{free-fit}} - a_{0\_ms1}^{\text{free-fit}}$

CD a_2</td></tr>
<tr><td>23</td><td rowspan="4">PV LWIR electronic cross-talk</td></tr>
<tr><td>24</td></tr>
<tr><td>25</td></tr>
<tr><td>27</td></tr>
<tr><td>28</td><td rowspan="2">Corrected a_0; CD a_2</td></tr>
<tr><td>29</td></tr>
<tr><td>30</td><td>2003 a_0a_2; $a_{0\_ms1} = 0$</td></tr>
<tr><td>31</td><td rowspan="6">Entire mission MS corrected a_0

CD a_2</td><td rowspan="6"></td><td rowspan="2">$a_0 = 0$
CD a_2</td><td></td></tr>
<tr><td>32</td><td rowspan="5">PC LWIR optical cross-talk</td></tr>
<tr><td>33</td><td rowspan="4">Early mission: MS corrected a_0
Since 2003: $a_0 = 0$
CD a_2</td></tr>
<tr><td>34</td></tr>
<tr><td>35</td></tr>
<tr><td>36</td></tr>
</table>

2. MODIS TEB CALIBRATION ALGORITHM BACKGROUND

2.1 MODIS TEB calibration algorithm

MODIS TEB includes mid-wave infrared (MWIR) bands 20-25, covering a wavelength range from 3.8 to 4.5 μm, and long-wave infrared (LWIR) bands 27-36, from 6.8 to 14.2 μm. All the MWIR and LWIR bands 27-30 consist of ten PV detectors per band, while the LWIR bands 31-36 consist of ten PC detectors per band. The on-board BB serves as the primary calibration source, while the space view (SV) provides an instrument background reference. Normally, this temperature is set to 290 K and 285 K for Terra and Aqua MODIS, respectively. Starting April 2020, the Terra BB temperature setpoint has been changed to 285 K. The MODIS TEBs calibration uses a quadratic calibration algorithm on a scan-by-scan basis for each TEB detector and scan mirror side. The linear coefficient of the response function is calibrated scan-by-scan using a two-point calibration performed via the response to the on-board BB referenced to the SV, and the non-linear and offset terms coming from a LUT. The BB warm-up and cooldown (WUCD) operation is used to characterize and update the instrument non-linear response coefficients on-orbit. Every WUCD operation is performed quarterly, and the BB temperature varies from instrument ambient temperature (about 270 K) to 315 K.
The calibration radiance (L_{CAL}) from the BB view is defined as:

$$L_{CAL} = RVS_{BB}\varepsilon_{BB}L_{BB} + (RVS_{SV} - RVS_{BB})L_{SM} + RVS_{BB}(1 - \varepsilon_{BB})\varepsilon_{cav}L_{cav}, \quad (1)$$

where ε is the BB or cavity (cav) emissivity, L is the BB, scan mirror (SM), or cavity radiance, and RVS is the response-versus-scan-angle at the SV or BB view. The TEB calibration is based on a quadratic algorithm that converts the digital response of the sensor to calibration radiance (L_{CAL}):

$$L_{CAL} = a_0 + b_1 dn_{BB} + a_2 dn_{BB}^2, \quad (2)$$

where a_0 and a_2 are the offset and non-linear coefficients, and dn_{BB} is the BB's digital response. Equations (1) and (2) are used for both the WUCD and scan-by-scan linear coefficient calibrations during nominal operation. The scan-by-scan linear coefficient, b_1, can be calculated using the emissivity, RVS, and nonlinear coefficients LUTs:

$$b_1 = [L_{CAL} - a_0 - a_2 dn_{BB}^2]/dn_{BB}. \quad (3)$$

Using the calibration coefficients for each detector and scan mirror side, EV radiance retrievals can be performed by:

$$L_{EV} = \frac{1}{RVS_{EV}}[a_0 + b_1 dn_{EV} + a_2 dn_{EV}^2 - (RVS_{SV} - RVS_{EV})L_{SM}], \quad (4)$$

where RVS_{EV} is the EV RVS as a function of mirror AOI. The MODIS TEBs RVS come from pre-launch tests and have been verified and monitored post-launch using pitch maneuvers. A detailed description on the MODIS TEB calibration is described by Xiong et al. [1].

The calibration assessment can be performed using L1B data over selected Earth scenes. Since the on-board BB temperature is from approximate 270K to 315K, the a0 uncertainty is relatively large and thus the a0 uncertainty has larger impact on the measurement over cold scenes. Deep convective clouds (DCC) have been proven to be useful Earth scenes for the calibration assessment of the MODIS TEBs. In order to remove solar reflectance effects on the measurements of MWIR bands and assess the calibration at low BTs, Quasi-deep convective clouds (qDCC), which are the DCC during nighttime, are used [6]. From the MODIS TEB calibration algorithm, the calibration uncertainty impact on the L1B product can be modeled analytically. A detailed description on the development and application of this technique to DCC is described by Chang et al. [6]. One practical application is to use the model to evaluate mirror side, detector, or bias differences. It can also be utilized to assess long-term stability. Thus, the calibration uncertainty impact on the L1B product can be modeled, and an a_0 correction for mirror side or bias differences can be derived.

2.2 MODIS TEBs electronic crosstalk

Signal contamination in the form of electronic crosstalk has been observed in many of the TEBs since pre-launch. This became particularly evident for Terra MODIS bands 27 − 30 after the instrument underwent a safe mode event in February 2016, for which a correction was applied in C6.1 shortly after [3, 4]. Moreover, the some of the detectors in Terra MODIS MWIR bands also show signs of electronic crosstalk contamination, which can be seen clearly from the Moon observations. The signal contamination alignment for band 22 detector 8 and band 23 detector 10 is illustrated in Fig. 2.2-1. Several anomalous peaks due to contamination from detectors in bands 20, 21, 23, 24 and 26 outside

of the main lunar signal, which is cut off at the top of Figs. 2.2-1a and 2.2-1b, can be easily seen. These anomalous peaks represent crosstalk contamination. Furthermore, these electronic crosstalk effects can potentially impact the L1B and higher-level products, causing image artifacts such as striping and radiometric biases.

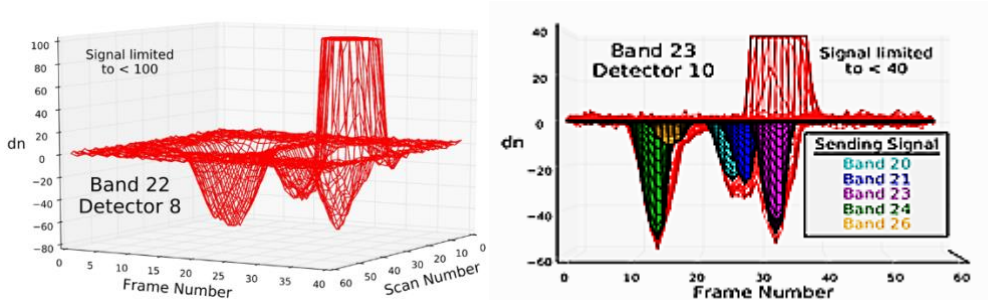

(a) (b)

Figure 2.2-1: Example of contamination data around the main lunar signal. The data for these plots are from the Terra MODIS lunar observation on May 26, 2016.

Generally, crosstalk occurs between bands and detectors that are located on the same FPA (Fig. 2.2-2). The source of the contaminating signals can be identified using lunar data. There are two kinds of crosstalk . One is detector 1 contamination from detector 10 of a sending band, as shown in Fig. 2.2.-2 (a). The second is band-to-band among MWIR bands or among PV LWIR bands, as shown in Fig.2.2-2 (b). The contaminating signal has been assumed to be linearly proportional to the measured signal from the identified sending bands. Since electronic crosstalk affects the digital signal in each data sector, it will have an impact on background signal as well as the signal from any measured EV or on-board calibrator (OBC) scene. However, since the background contamination is at a nearly constant level, this contamination can be subtracted off with the rest of the background signal. In a simplistic fashion, the crosstalk coefficients, $c_{i,j}$, are in the form of a matrix which contains linear coefficient values that connect a detector's receiving contamination (*i*), to each of the detectors that send contamination (*j*). The correction is applied to the background-subtracted digital counts (*dn*) for each data sector in order to derive the calibration coefficients and EV scene radiance. Thus, the corrected signal on the pixel level can be written as:

$$dn_i(S,F) = dn_i^*(S,F) - \sum_j c_{i,j} dn_j^*(S,F+\Delta F_j) \qquad (5)$$

Here, S and F represent the scan and frame numbers, respectively, ΔF_j is the relative frame offset of detector j with respect to detector i, and the * represents the digital counts before the application of the correction. A detailed description of the correction and its impact on the L1B data is described by Wilson et al. [4], and in the 2018 MODIS TEB electronic crosstalk workshop [5].

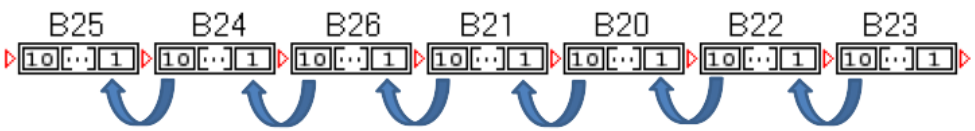

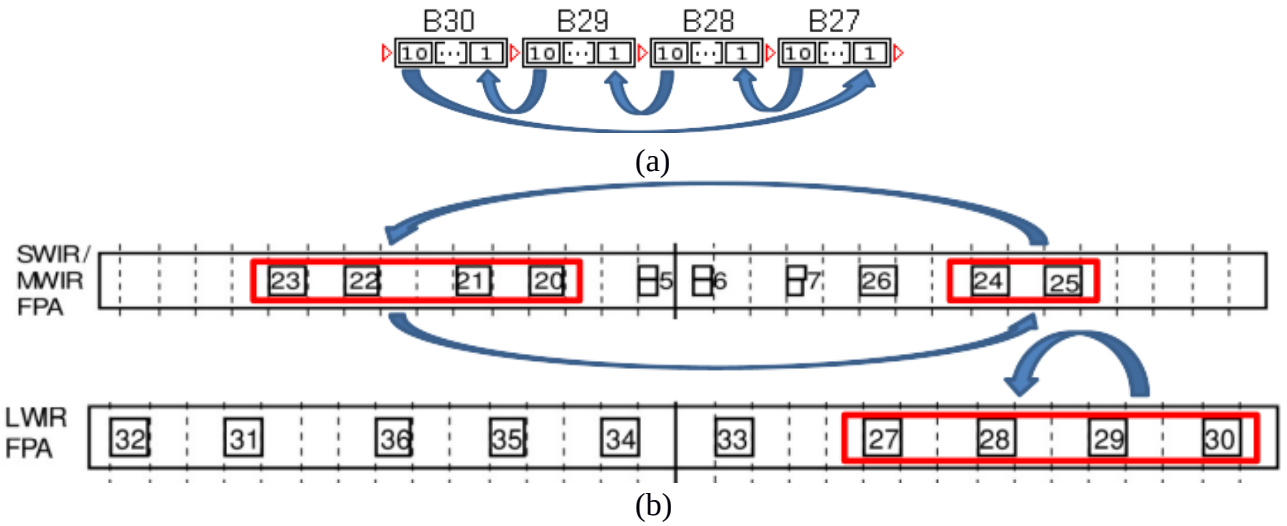

Figure 2.2-2: MODIS TEBs (a) detector-to-detector and (b) band-to-band crosstalk contamination schematic.

3. RECOMMENDATIONS FOR THE TERRA MODIS TEB

3.1 MWIR electronic crosstalk correction

A crosstalk correction for selected detectors of the Terra MWIR bands will be applied in C7. Each detector that was selected for correction underwent extensive evaluation of the correction's impact on the L1B product and image quality. Figure 3.1-1 displays an example of the electronic crosstalk correction coefficients application on the L1B product for band 24. It can be clearly seen from the images, BT profiles, and BT histograms that the application of the electronic crosstalk coefficients effectively removes striping and brings the corrected detectors in-family with the other detectors. Ultimately, it was decided that only 4 detectors (band 22 detector 8, band 23 detectors 1 and 10, and band 24 detector 1) in the Terra MWIR bands have contamination levels that require a correction in the L1B product (Table 3.1-1). Figure 3.1-2 illustrates the Terra MODIS C7 MWIR electronic crosstalk correction coefficients mission-long trends for the selected detectors and bands, respectively. All other detectors have either small levels of contamination or the correction is not significant enough - when compared to the normal variation of the bands' BT retrievals. These results and conclusions were presented in August 2018 in a workshop hosted by MCST at the MODIS Sensor Working Group (MsWG) meeting referred to as the MODIS Thermal Emissive Band Crosstalk Workshop [5].

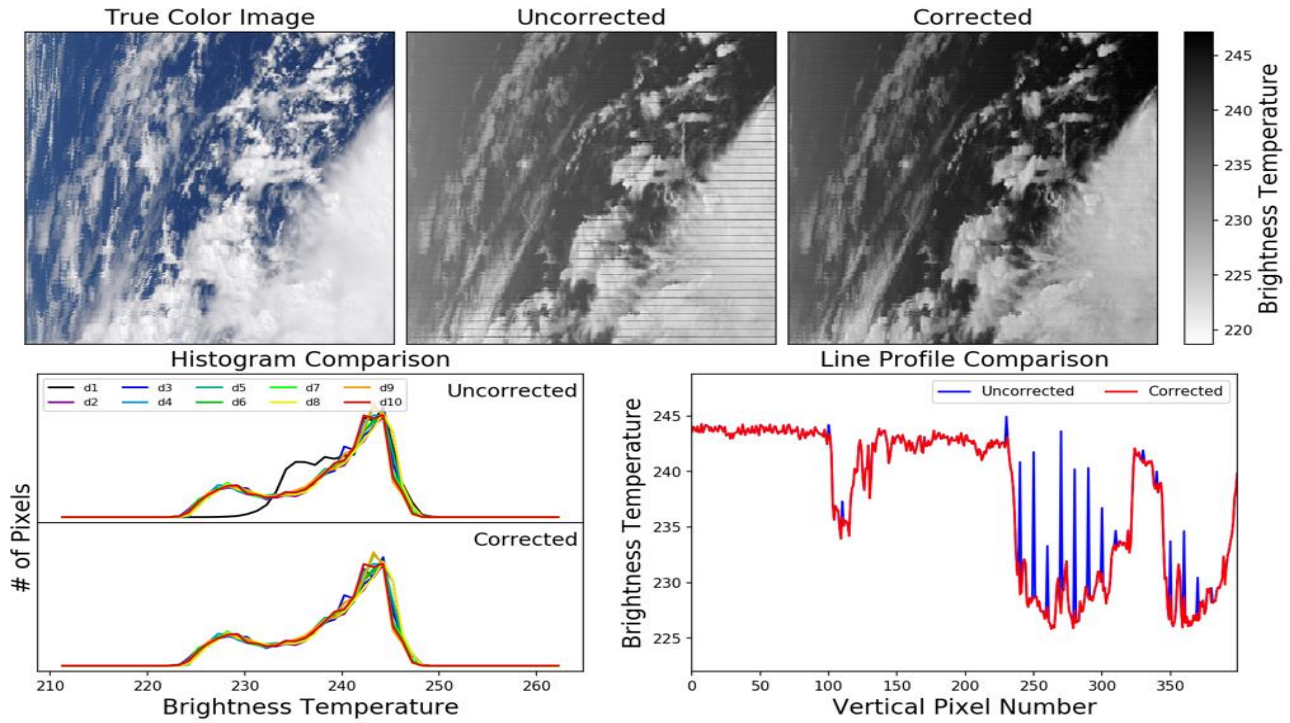

Figure 3.1-1: Crosstalk correction example for Terra MODIS band 24. (Top) True color, uncorrected, and corrected images. (Bottom left) Histogram comparisons for the selected scene before and after the electronic crosstalk correction is applied. (Bottom right) Vertical line profiles comparison through the center frame of the selected scene.

Table 3.1-1 Terra MODIS MWIR bands and detectors selected for electronic crosstalk correction in C7.

Band	Detector	Contamination Impact
22	8	Large striping over ice cloud scenes and water scenes (~0.5K).
23	1,10	Large striping over ice cloud scenes and water scenes (~0.5K).
24	1	Striping over ice cloud scenes and 0.5 -1 K change over ocean scenes

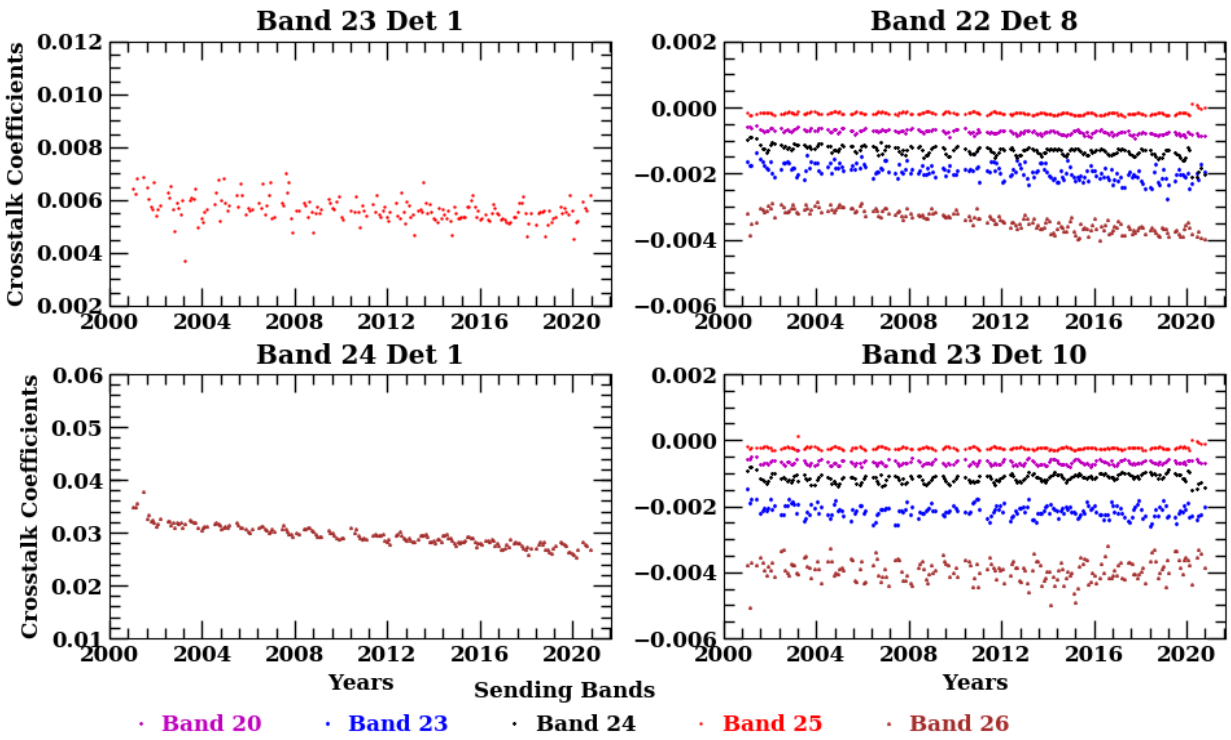

Figure 3.1-2: Terra MODIS C7 MWIR electronic crosstalk correction coefficients mission-long trends for the selected detectors and bands. The left two plots show the crosstalk coefficients trending for detector 1 of bands 23 and 24 with sending signal from detector 10 of sending band. The right two plots show coefficients for 2 selected detectors with the contaminations are from band-to-band crosstalk .

3.2 Band 30 stability improvement

Inter-sensor comparisons and vicarious calibration approaches have confirmed that the Terra band 30 BTs have been drifting downward [7-11]. This has been observed both through the Terra MODIS-Infrared Atmospheric Sounding Interferometer (IASI) time series (2007-2019) and MODIS mission-long EV trending results over qDCC, Dome Concordia (Dome-C), and the ocean (Figs. 3.2-1 and 3.2-2). These biases are larger for lower BT scenes. To solve for this artifact, for both the Dome-C site and an ocean location in the Bahamas, one month's worth of EV data for every year of the Terra MODIS mission was re-processed using the a_0 and a_2 calibration coefficients from the 2003 LUT after the instrument's last configuration change. Comparison tests between these coefficients and C6.1 demonstrated significant reduction in bias for both Earth scenes. Figure 3.2-3 illustrates the C7 bias corrections for the Dome-C and ocean targets. Thus, Terra MODIS C7 will use the a_0 and a_2 calibration coefficients from the 2003 LUT (after last configuration change) to re-process Terra MODIS band 30 for the instrument's entire mission. Moreover, the Dome-C, ocean, and qDCC Earth scenes will continue to be monitored for bias changes in C7.

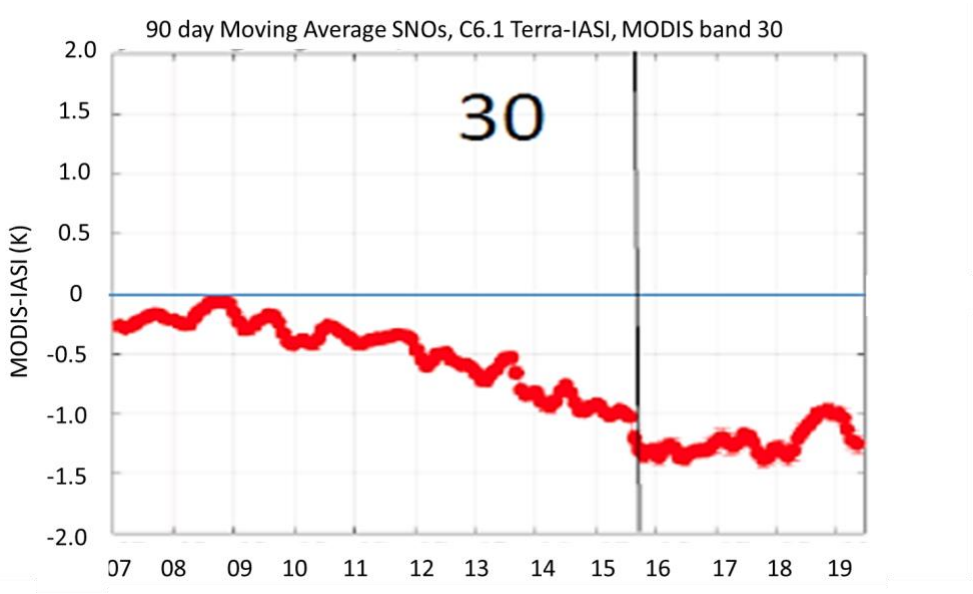

Figure 3.2-1. Terra MODIS-IASI biases for Terra MODIS band 30 from the years 2007 to 2019. This is for C6.1. (Source: Chris Moeller)

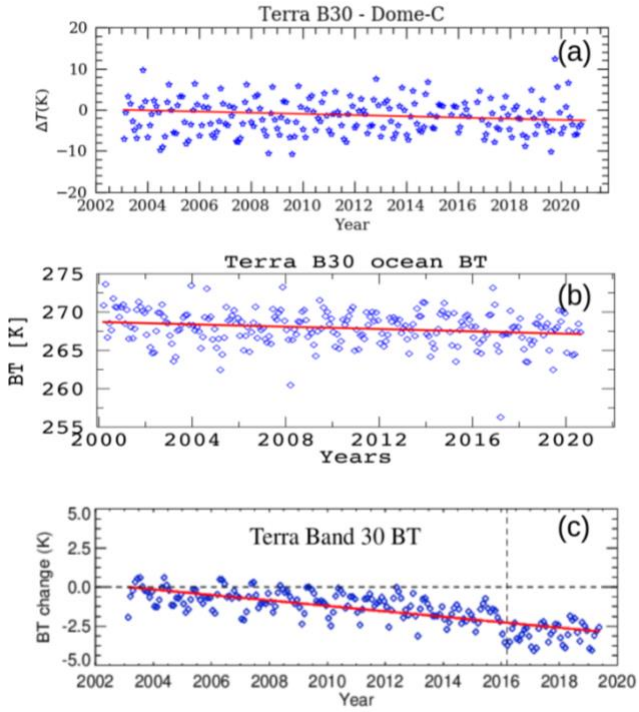

Figure 3.2-2. Terra MODIS mission-long retrievals over (a) Dome-C, (b) the ocean, and (c) qDCC for band 30. Blue markers represent monthly-averaged data. Red lines define data's fit. This is for C6.1.

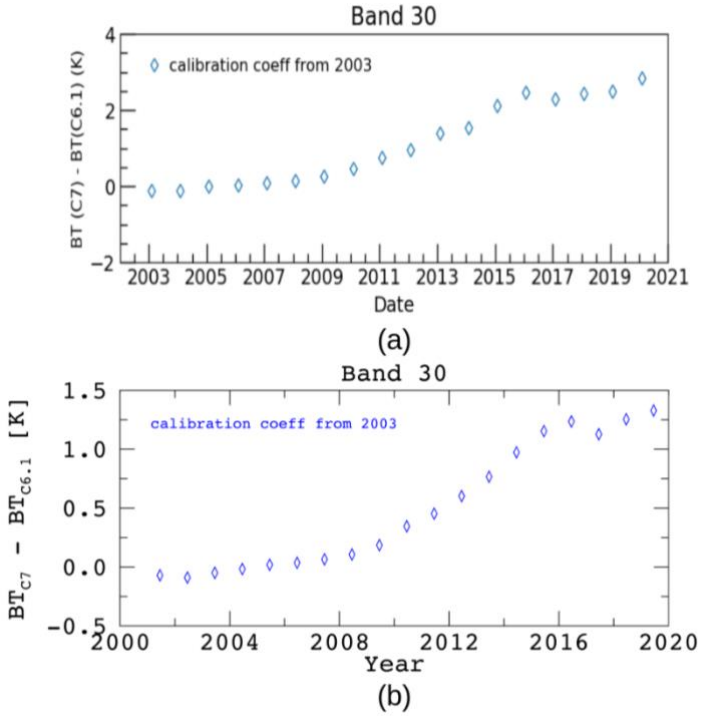

Figure 3.2-3. Terra MODIS C7 band 30 bias corrections (compared to C6.1) for the (a) Dome-C and (b) ocean targets. Blue markers represent monthly-averaged data.

3.3 Bands 20 and 29 cold scene bias correction

When compared to the IASI instrument, part of the payload of the MetOp series of polar-orbiting meteorological satellites, Terra MODIS has shown cold scene biases for some TEBs, as demonstrated by Moeller et al. [7]. This has been further confirmed by MCST in separate efforts [8]. Figure 3.3-1 displays the cold scene biases for Terra MODIS bands 20 and 29 when compared to IASI from the years 2007 to 2019. For band 20, warm scenes show quite stable trends. However, band 29 shows a slight, upward trend for the warmer scenes. In order to solve for these biases, a similar strategy to the one discussed in Section 2.3 was used, where the BT-dependent biases are estimated using the Terra MODIS-IASI difference at 200 K from 2007-2019, and the trends of the biases are obtained from MODIS retrievals over qDCC. Figure 3.3-2 illustrates the Terra MODIS mission-long retrievals over qDCC, Terra-IASI biases over qDCC, and a0 corrections for bands 20 and 29. Using the MODIS retrievals over qDCC referenced to the Terra-IASI biases, an a_0 correction is derived for each month of data. This a_0 correction, as well as the free-fitted a_2, are calculated using a yearly-averaged sliding window. Because Terra MODIS underwent several configuration and setting changes from the years 2000 to 2003, the average a_0 correction from 2003-2004 is used for band 20 over this early mission period to avoid discontinuity. Moreover, after every WUCD operation, an a_0 correction is applied to both mirror sides and a_2 is computed. Before C7 is implemented, the Terra MODIS C6.1 qDCC trends and Terra-IASI biases will be processed to maintain continuous a_0 corrections. After its implementation, the C7 L1B will be used to monitor the qDCC and bias trends. Furthermore, Dome-C, ocean, and desert measurements will also be used as reference to monitor a broader BT range.

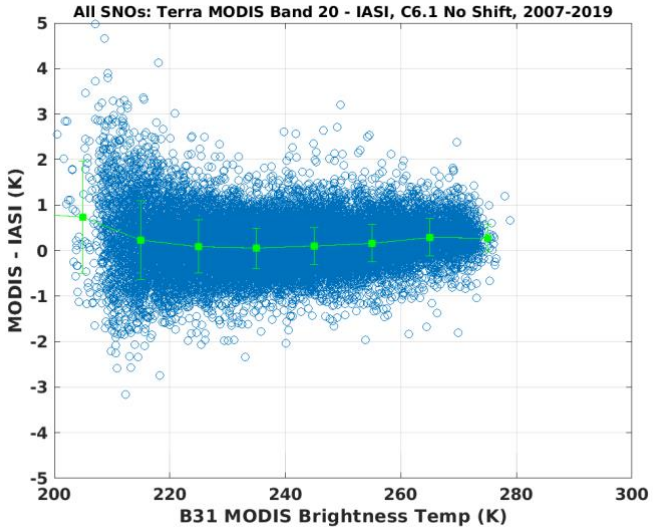

(a)

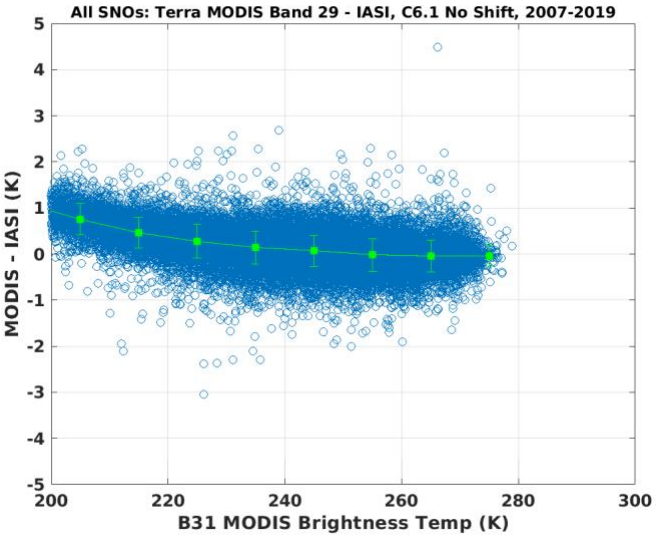

(b)

Figure 3.3-1. Terra MODIS-IASI biases for Terra MODIS bands (a) 20 and (b) 29 from the years 2007 to 2019. (Source: Chris Moeller)

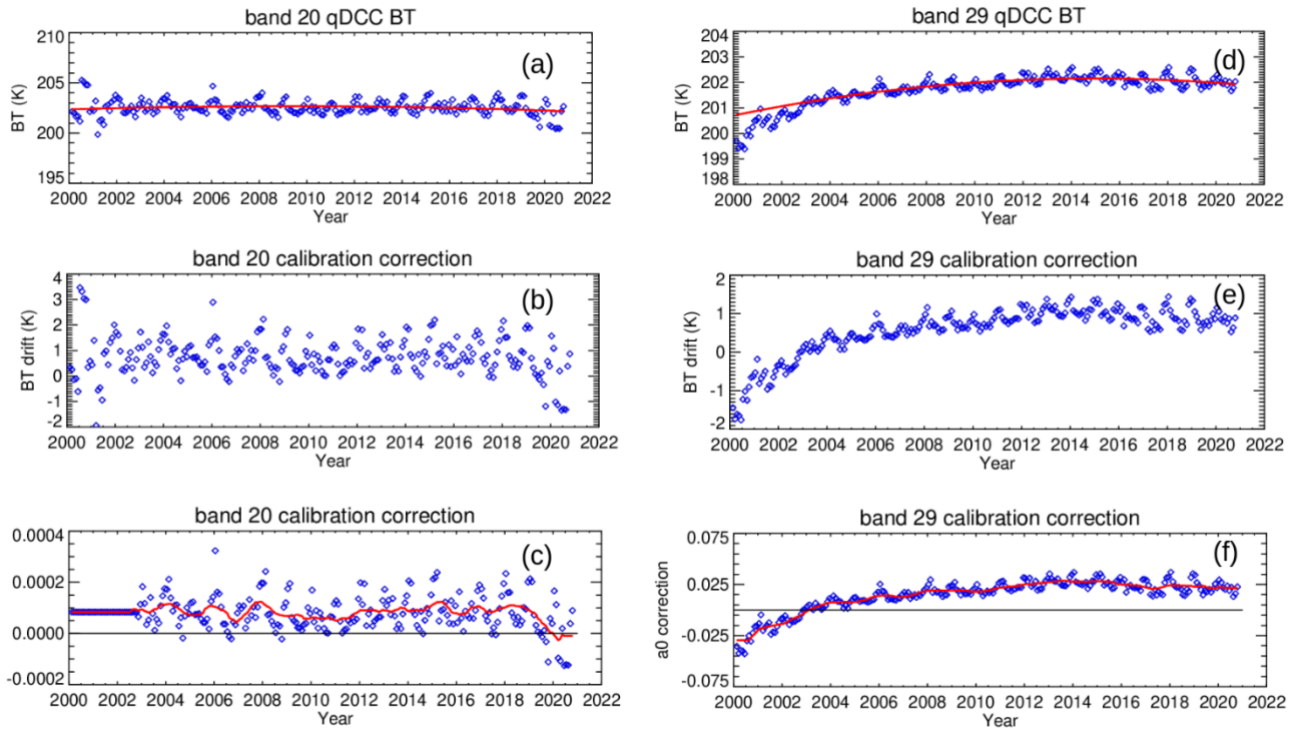

Figure 3.3-2. Terra MODIS mission-long retrievals over qDCC (a and d), Terra-IASI biases over qDCC (b and e), and a0 correction (c and f) for bands 20 and 29. Blue markers represent monthly-averaged data. Red lines define data's fit in (a) and (d) and yearly moving average in (c) and (f).

3.4 Early mission PC bands mirror side difference correction

Early in the Terra MODIS mission (2000-2002), the instrument underwent several instrument setting and electronic configuration changes (Table 3.4-1). Hence, the instrument response was affected after each change and, consequently, the calibration data shows relatively larger uncertainty when compared to that after the year 2003. The mirror side differences were analyzed for each TEB and each time interval between these changes, and assessments over qDCC and Dome-C show relatively larger mirror side differences and discontinuities for low BT measurements. MCST performed several analyses and found that re-processing the C7 LUTs to accommodate for new timestamps - more representative of each setting and configuration change - improves the calibration consistency and accuracy by generating LUTs for each change period. The PV bands mirror side differences were mostly reduced. However, because a_0 is set to zero for both mirror sides for the PC bands, the mirror side differences remained. Figure 3.4-1 illustrates the Terra MODIS early mission mirror side BT differences for bands 34 (~ 0.5 K) and 36 (~ 0.8 K). Thus, MCST analyzed the mirror side BT differences using cold scenes and derived an a_0 correction associated with the mirror side differences for PC bands 33-36. This a_0 correction is used to generate the C7 a_0 and a_2 LUTs between 2000 and 2003. Lastly, Fig. 3.4-2 shows the Terra MODIS mirror side BT difference comparison as a function of BT between C7 and C6.1 for bands 34 and 36 using the LUTs from the WUCD operation that happened on October 27th, 2001. The cross-comparison between C7 and C6.1 demonstrates mirror side BT difference corrections of 0.5 K and 0.7 K at 200K for bands 34 and 36, respectively.

Table 3.4-1. Terra MODIS setting and configuration changes from 2000 to 2002.

Date	Changes
06/08/00	Cold focal plane assembly stopped controlling temperature
10/30/00	MODIS switches to B-side electronics configuration
07/02/01	MODIS switches to A-side electronics configuration using PS1
03/19/02	Spacecraft safe mode anomaly during maneuver
09/17/02	Switch to B-side formatter; other components remain on A-side

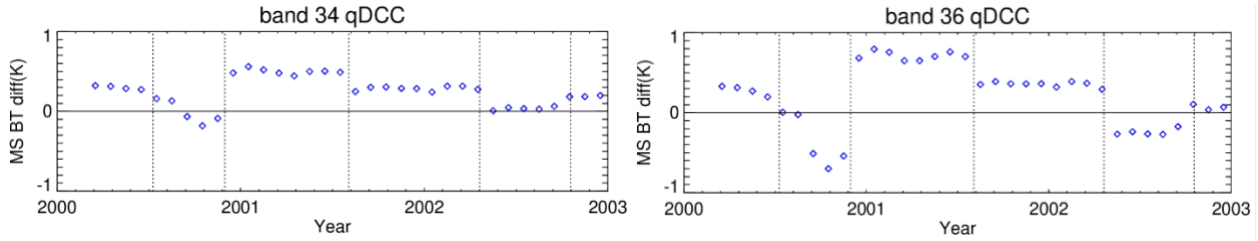

(a) (b)

Figure 3.4-1. Terra MODIS early mission mirror side BT differences for bands (a) 34 and (b) 36. Blue markers represent monthly-averaged data.

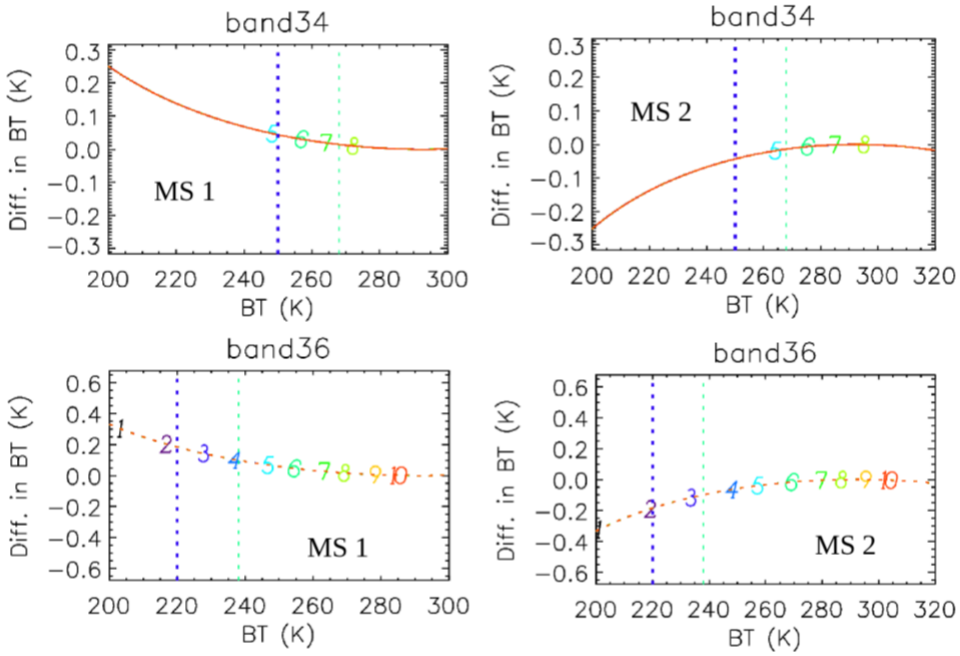

Figure 3.4-2. Terra MODIS mirror side BT difference comparison as a function of BT between C7 and C6.1 for bands 34 and 36 using the LUTs from the WUCD operation that happened on October 27th, 2001.

4. RECOMMENDATIONS FOR AQUA MODIS TEB

4.1 Aqua MWIR and LWIR electronic crosstalk correction

Aqua MODIS C7 will introduce electronic crosstalk correction coefficients for selected detectors in the PV TEBs. Signatures of electronic crosstalk contamination are seen in lunar images by various Aqua MODIS bands from both the MWIR and LWIR FPAs. MCST spent substantial effort on surveying lunar images from scheduled lunar observations to determine all the bands and detectors affected by electronic crosstalk artifacts, and linked these with their respective sending bands and detectors. Moreover, linear crosstalk correction coefficients were developed from Moon observations for the pertinent bands/detectors and the entire Aqua MODIS mission. Afterwards, these were used to generate corrected L1B images and assess the impacts of electronic crosstalk on imagery. A detailed description of the correction and its impact on the L1B data is described by Keller et al. [12,13].

After various analyses and tests on the electronic crosstalk correction impacts on the L1B product, MCST proposes to apply electronic crosstalk corrections to selected detectors in the Aqua C7 PV bands. These results and conclusions were also presented in August 2018 in the MODIS Thermal Emissive Band Crosstalk Workshop [5]. Table 4.1-1 summarizes the detectors and bands selected for electronic crosstalk correction in Aqua MODIS C7. Figure 4.1-1 illustrates the Aqua MODIS C7 MWIR and LWIR electronic crosstalk correction coefficients mission-long trends for some selected detectors and bands, respectively. Generally, all coefficients are stable throughout the entire Aqua MODIS mission. However, the receiving band 30, detector 1 (sending band 29, detector 10) coefficients exhibit a slight, downward trend. Lastly, Figures 4.1-2 and 4.1-3 show examples of the electronic crosstalk correction coefficients application on the L1B product for bands 24 and 30. The L1B images displayed correspond to granules from October 11th, 2019. The electronic crosstalk corrections are applied to detector 1 (product order (P.O.)) for all the bands described in Table 4.1-1. Only band 29 will undergo additional electronic crosstalk correction for detectors 2 and 6 (P.O.). It can be inferred from the images, BT profiles, and BT histograms indicate that the application of the electronic crosstalk coefficients effectively removes striping and brings detector 1 in-family with the other detectors for all bands (more apparent for band 24, whose electronic crosstalk coefficients are larger (~4%) than for the other bands (<2%)).

Table 4.1-1. Aqua MODIS PV bands and detectors selected for electronic crosstalk correction in C7.

Band	Detector	Contamination Impact
20	1	Striping over some scenes (~0.15K).
22	1	Striping over some scenes (~0.20K).
23	1	Large striping over ice cloud scenes and water scenes (~0.5K).
24	1	Striping over low BT scenes during daytime.
25	1	Striping over some scenes (~0.20K).
27	1	Large striping over some scenes (~0.80K).
29	1,2,6	Striping over some scenes (~0.3K).
30	1	Striping over some scenes (~0.45K).

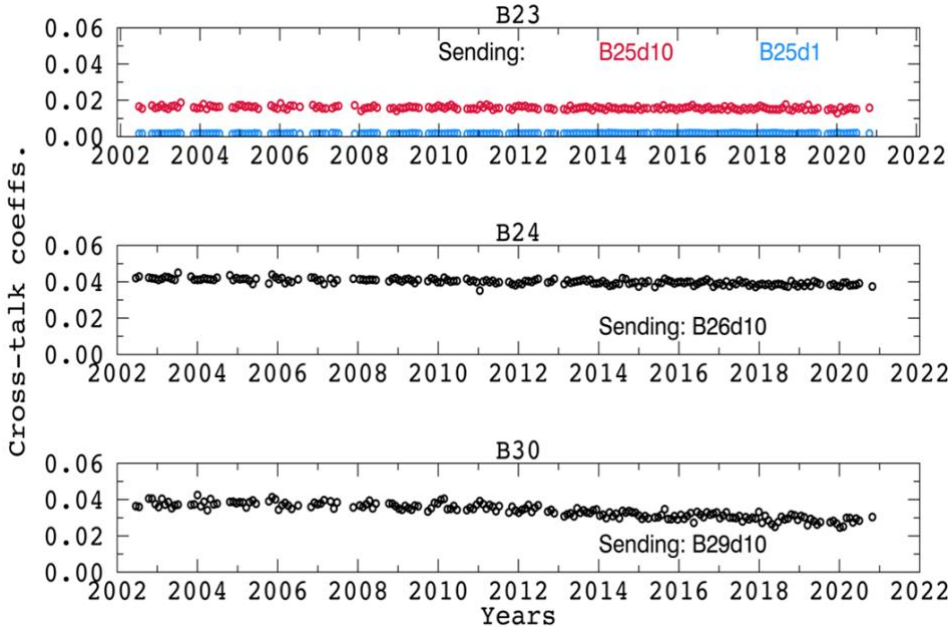

Figure 4.1-1. Aqua MODIS C7 electronic crosstalk correction coefficients mission-long trends for bands 23, 24, and 30.

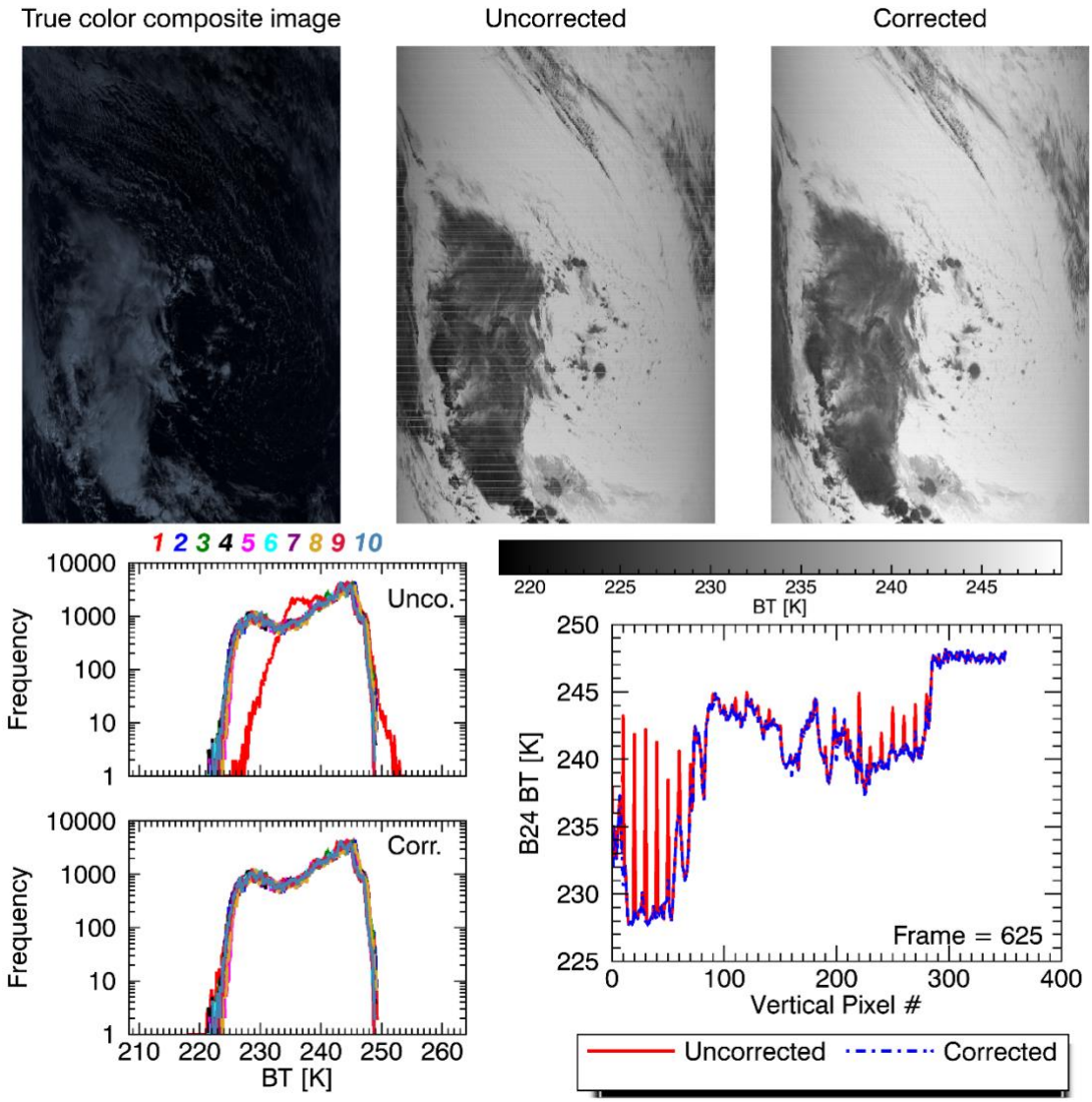

Figure 4.1-2. Electronic crosstalk correction coefficients application on the L1B product example for band 24, detector 1 (P.O.). The L1B images displayed correspond to a granule from October 11th, 2019.

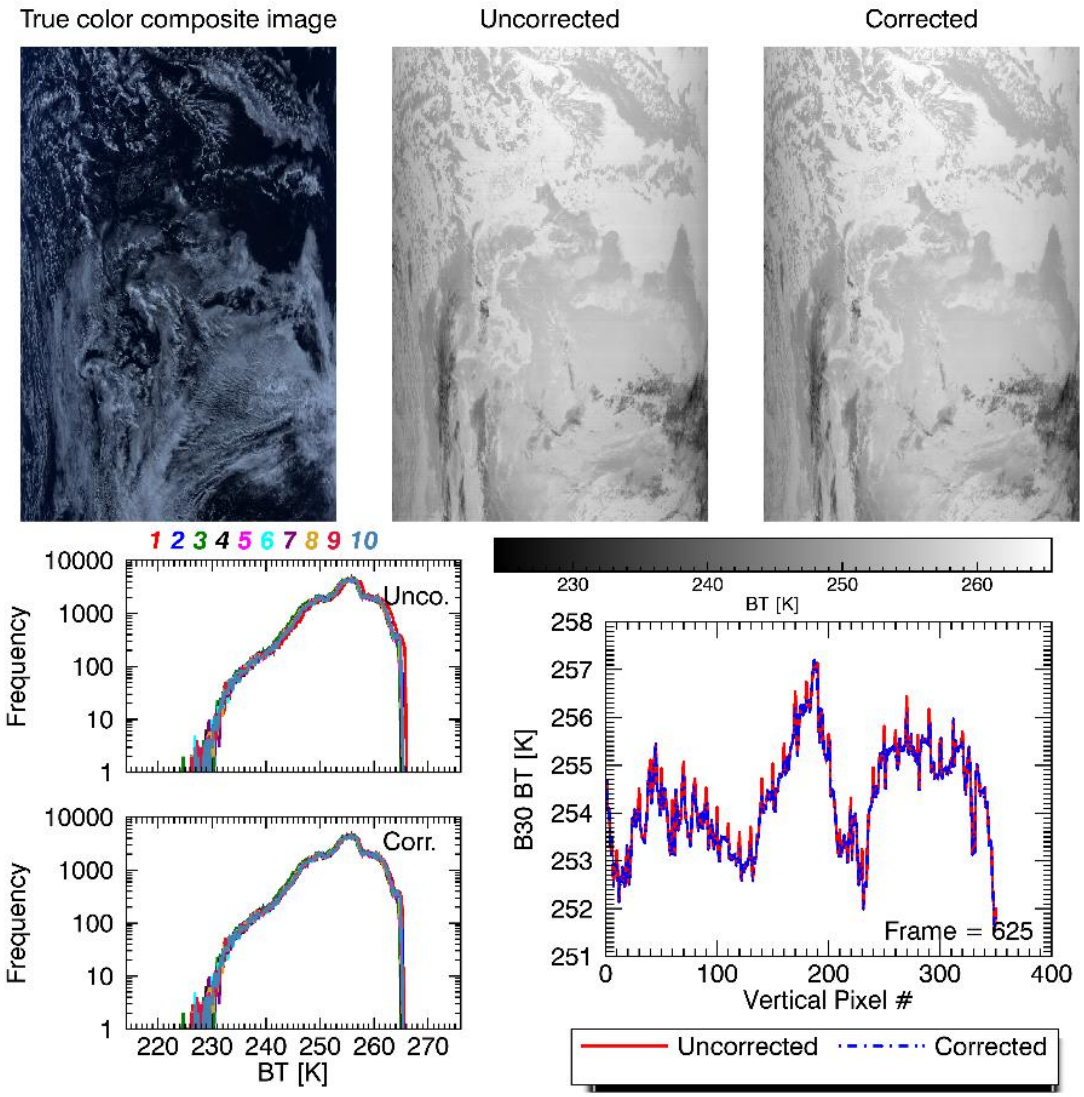

Figure 4.1-3. Electronic crosstalk correction coefficients application on the L1B product example for band 30, detector 1 (P.O.). The L1B images displayed correspond to a granule from October 11th, 2019.

4.2 Mission-long mirror side difference correction for all TEBs

As shown in Table 1.1-1, the pre-launch a_0 is used for Aqua PV bands 20-25 and 27-30, while a_0 is set to zero for PC bands 31-36. After the Aqua MODIS mission-long mirror side BT differences were analyzed using qDCC, the formatter reset event (January 2018) was found to have caused significant mirror side difference changes. Therefore, as the methodology presented in Section 2.3, qDCC were used to assess the instrument changes and associate the mirror side differences to an a_0 correction. The method was applied to all the MODIS TEBs (except bands 21 and 31). Figure 4.2-1 illustrates the Aqua MODIS mission-long mirror side BT differences for MWIR bands 20-25. Band 20 has the largest mirror side BT difference (approximately 1.8 K) before the formatter reset. After the reset, this mirror side difference is significantly reduced (decreased to 0.5 K). The other MWIR TEBs also show up to a 1-K mirror side BT difference before the formatter reset event. Because band 21 uses a linear

calibration algorithm with a0 and a2 set to zero, its mirror side BT differences are not directly comparable to the other bands. Before and after the formatter reset, the band 21 mirror side BT differences change direction. For all other TEBs, the mirror side differences are smaller after the reset.

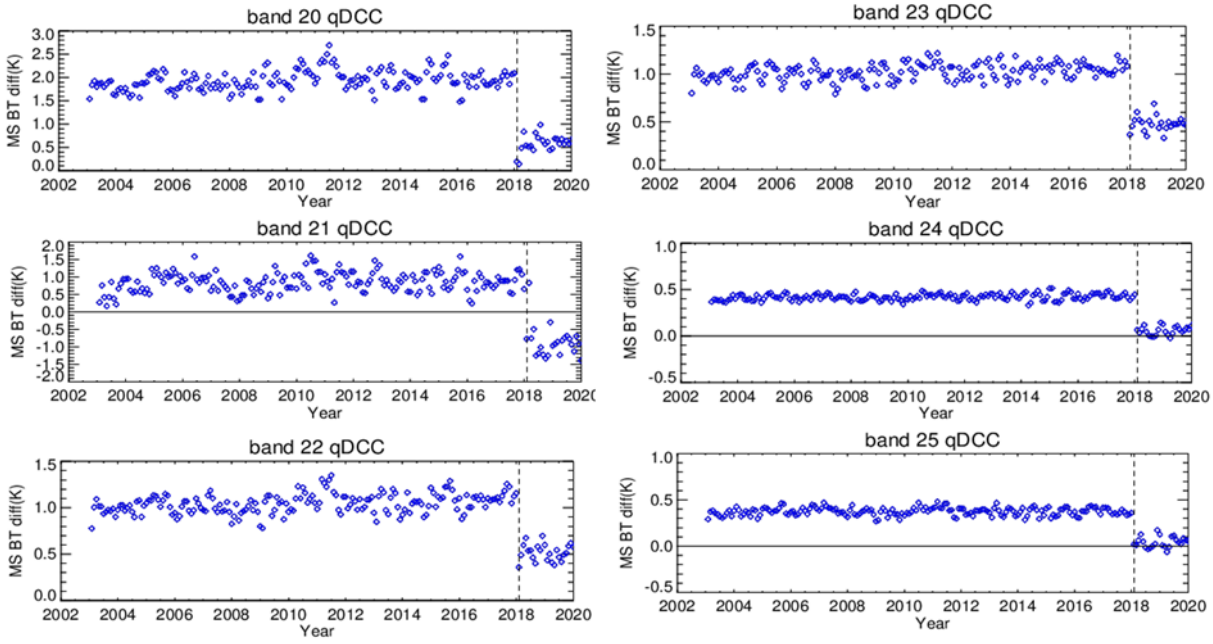

Figure 4.2-1. Aqua MWIR bands 20-25 long-term mirror side BT differences over qDCC. Each symbol represents monthly-averaged mirror side differences. The vertical dashed line indicates the time of occurrence for the formatter reset (January 2018).

Figure 4.2-2 displays the Aqua MODIS mission-long mirror side BT differences for PV LWIR bands 27-30. Band 27 has the largest mirror side difference among these four bands (approximately 0.8 K) before the formatter reset. Similar to the MWIR TEBs, after the reset, the mirror side differences for all four bands decreased significantly. Moreover, all four bands exhibit slight - and similar in pattern - mirror side difference fluctuations, suggesting that these are not noise. The PC LWIR TEBs mirror side differences are small and not shown here. Figure 4.2-3 shows the Aqua mission-long a_0 correction for all TEBs - except bands 21 and 31. A linear calibration is still applied to band 21 in C7, and thus the a_0 correction is not applied to this band. Band 31 is used as the reference band for the qDCC pixel identification process; hence no mirror side differences and no a_0 corrections are derived for this band. Moreover, band 31 exhibits accurate calibration and excellent stability. As such, its mirror side differences are expected to be negligible.

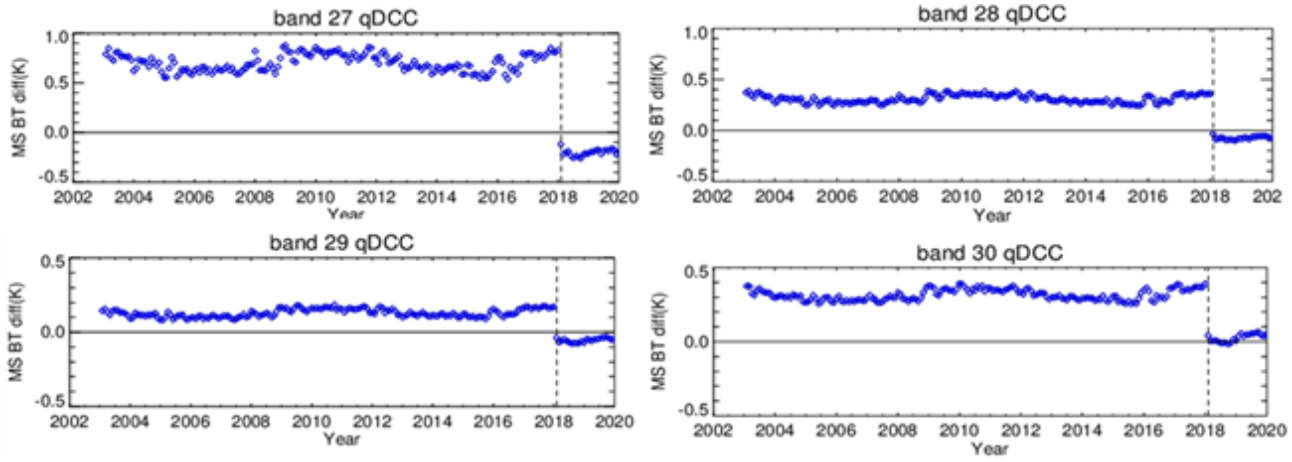

Figure 4.2-2. Aqua LWIR bands 27-30 long-term mirror side BT differences over qDCC. Each symbol represents the monthly-averaged mirror side differences. The vertical dashed line indicates the time of occurrence for the formatter reset (January 2018).

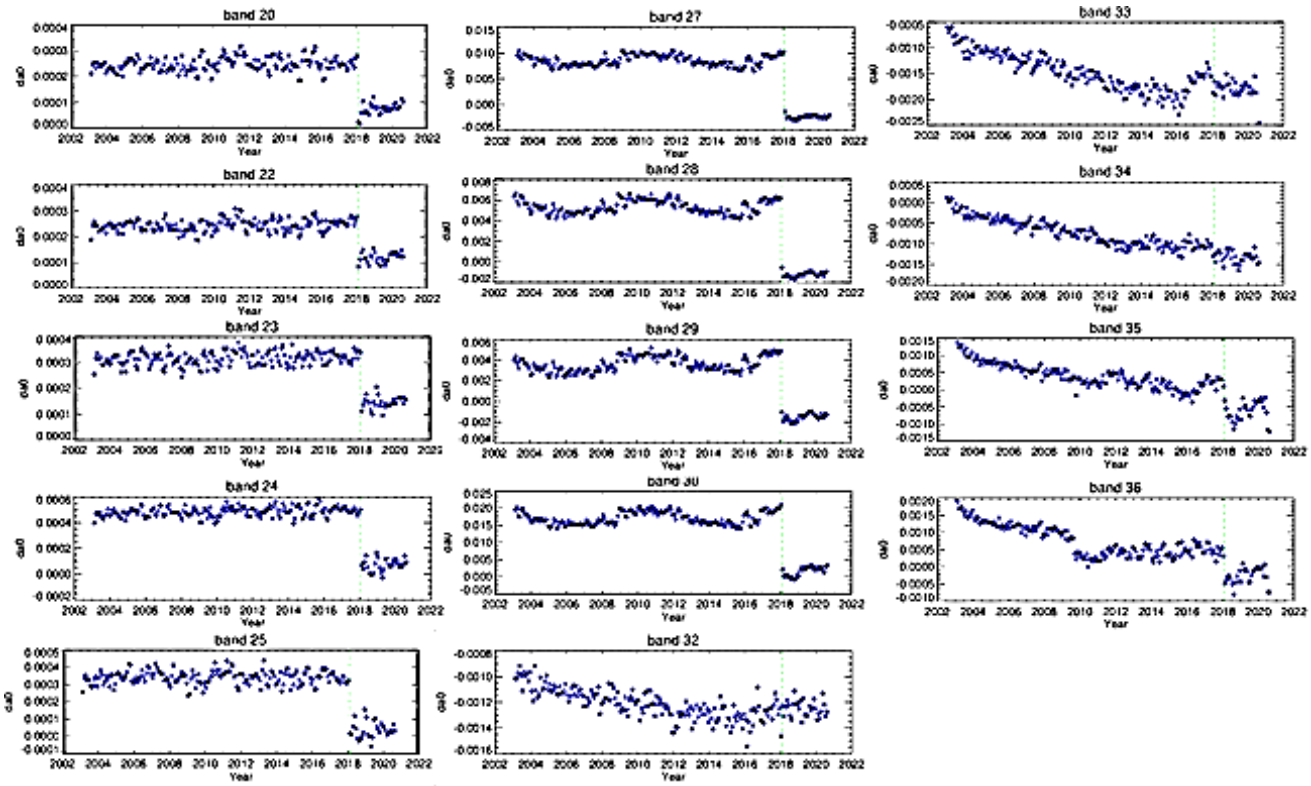

Figure 4.2-3. Aqua mission-long a_0 correction for all TEBs. Each symbol represents the monthly a_0 correction. The vertical dashed line indicates the time of occurrence for the formatter reset (January 2018).

After deriving the a_0 bias correction using extremely cold scenes (i.e. qDCC), a set of test LUTs (later on referred to as C7) were developed to evaluate their efficacy in reducing the Aqua MODIS TEBs mirror side differences when compared to C6.1. The C7 algorithm was slightly changed to the one currently employed in C6.1 by applying the derived bias correction (+½ to MS2, -½ to MS1) to the pre-launch a_0 coefficients and, afterwards, free-fitting the a_2 coefficients using the CD data from each WUCD operation. This is different from C6.1 in that the pre-launch a_0 coefficients used have no bias correction, and the a_2 coefficients are the pre-launch a_2 coefficients adjusted using an iteration procedure described by Wu et al. [2]. There was no algorithm change to the band 21 b_1 coefficients (linear fit with a_0 and a_2 equal to zero). Using C7 test LUTs, selected EV targets were evaluated by producing C7 test L1B data to compare with the official C6.1 L1B product. Figure 4.2-4 displays the mirror side BT differences between the C6.1 L1B and C7 test LUT L1B products for Aqua MODIS TEB 22, 23, 27, and 30. The MODIS retrievals are analyzed by cross-comparing with results from the AIRS instrument also onboard Aqua. All data are from September 17th, 2017. The results indicate significant reduction in mirror side differences for the bands shown. Moreover, all other bands covered by the AIRS wavelength spectrum demonstrated significant improvement as well. Furthermore, C7 test L1B data were generated for two months' worth of DCC data (one month - July 2017 - before and one month after - July 2018 - the formatter reset). These C7 L1B data were also compared with the C6.1 L1B product, and the results are summarized in Table 4.2-1. The test results demonstrate significant reduction in mirror side differences for all TEBs - especially for the Aqua MODIS TEBs in C6.1, whose mirror side differences are quite large. After the a_0 bias correction, these MS differences are greatly reduced. Likewise, PV LWIR bands 27-30 show substantial reduction in their MS differences after the correction. Lastly, while the mirror side differences for the PC LWIR bands in C6.1 are marginal, the correction still proves practical by making the biases smaller. A more detailed description of the MODIS TEBs calibration algorithm improvements for C7 is provided by Chang et al. [14].

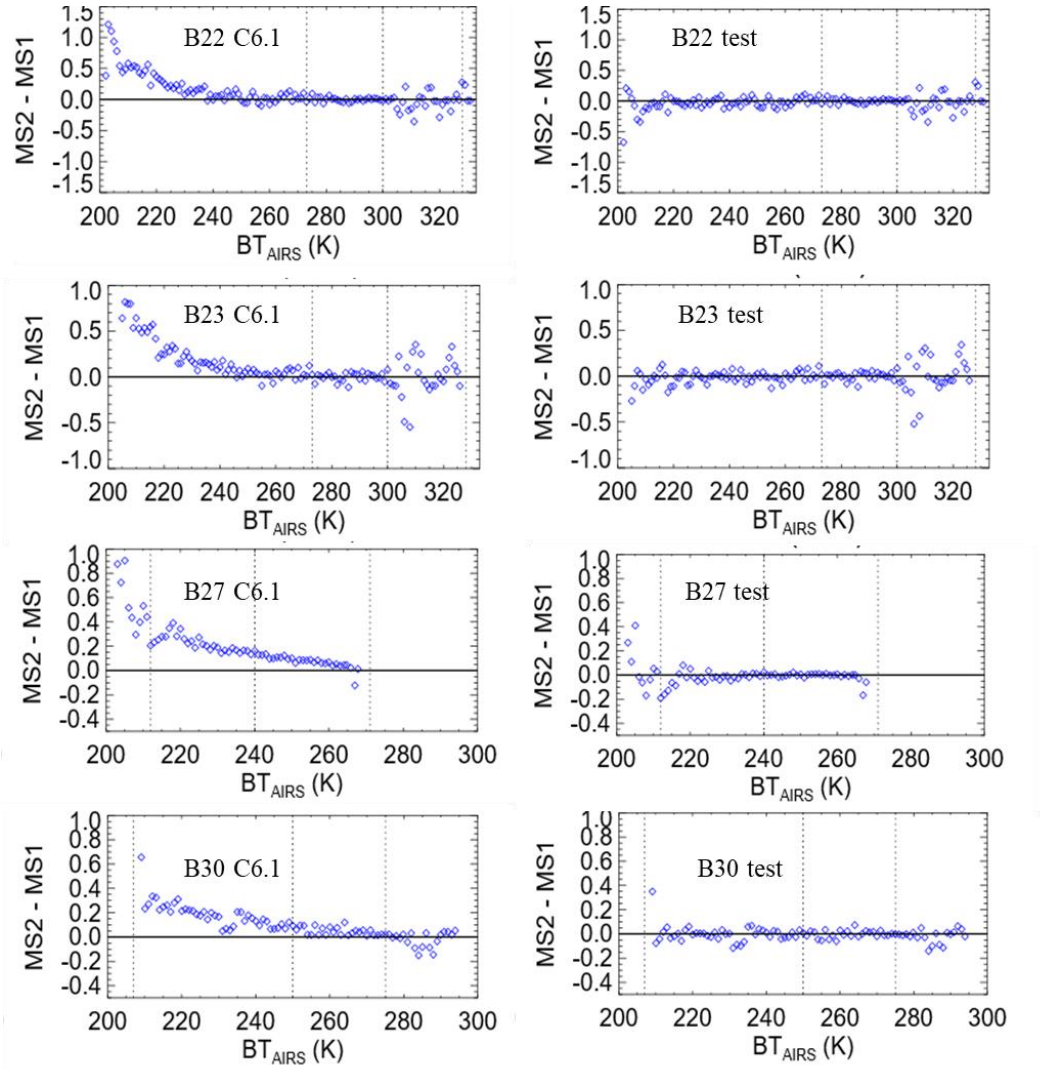

Figure 4.2-4. Aqua MODIS C6.1 L1B and C7 LUT L1B products mirror side BT differences for bands 22, 23, 27, and 30 using an Aqua MODIS-to-AIRS cross-comparison. All data are from September 17, 2017. (Left) C6.1 mirror side BT differences as a function of the AIRS BT for Aqua bands 22, 23, 27, and 30. (Right) C7 mirror side BT differences as a function of the AIRS BT for Aqua bands 22, 23, 27, and 30. The vertical dotted lines represent BTs at 0.3 of typical radiance, typical temperature, and maximum temperature for each TEB from left to right, respectively.

Table 4.2-1. Aqua C6.1 and C7 (test) LUT mirror side BT differences over DCC measurements one month before and one month after the Aqua formatter reset event.

Band	C6.1 qDCC BT (K) 07/2017	C6.1 MS BT diff.(K) 07/2017	C7 LUT MS BT diff.(K) 07/2017	C6.1 MS BT diff.(K) 07/2018	C7 LUT MS BT diff.(K) 07/2018
20	202.9	1.845	0.168	0.474	-0.252
22	203.5	1.227	0.042	0.514	-0.208
23	204.0	1.076	-0.045	0.456	-0.190
24	209.0	0.264	0.008	0.005	-0.068
25	205.0	0.385	0.015	-0.006	-0.120
27	199.5	0.978	-0.021	-0.284	-0.046
28	200.2	0.428	-0.005	-0.100	-0.016
29	200.9	0.192	-0.007	-0.083	-0.029
30	211.1	0.392	0.010	0.014	0.013
32	198.9	-0.029	0.002	-0.035	-0.007
33	201.2	-0.038	0.007	-0.048	-0.017
34	202.9	-0.022	0.003	-0.026	0.001
35	205.3	0.009	-0.005	-0.015	0.005
36	206.7	-0.011	0.004	-0.026	-0.007

5. SUMMARY

The MCST TEB group has proposed updates for C7 based on a thorough review of the C6.1 TEB LUT algorithm and delivery procedure, and calibration assessments using Earth scenes and sensor inter-comparisons. This document provides a point-by-point discussion associated with each proposed algorithm improvement. Based on the internal test results, MCST expects an improved radiometric accuracy and quality of the C7 L1B. This memo only includes the discussion pertaining to the changes proposed to the LUTs in C7. Moreover, all LUTs are expected to be reprocessed using the most recent data and procedures.

REFERENCES

[1] Xiong, X., A. Wu, B. N. Wenny, S. Madhavan, Z. Wang, Y. Li, N. Chen, W. Barnes, and V. Salomonson, "Terra and Aqua MODIS Thermal Emissive Bands On-Orbit Calibration and Performance", IEEE Transactions on Geoscience and Remote Sensing, vol. 53, issue 10, pp. 5709 - 5721, 2015.

[2] Wu, A., Z. Wang, Y. Li, S. Madhavan, B. N. Wenny, N. Chen, and X. Xiong, "Adjusting Aqua MODIS TEB nonlinear calibration coefficients using iterative solution," Proc. SPIE 9264, Earth Observing Missions and Sensors: Development, Implementation, and Characterization III, 92640R (2 December 2014); https://doi.org/10.1117/12.2069246.

[3] Sun, J., X. Xiong, Y. Li, S. Madhavan, A. Wu, and B. N. Wenny, "Evaluation of Radiometric Improvements With Electronic Crosstalk Correction for Terra MODIS Band 27", IEEE Transactions on Geoscience and Remote Sensing, vol. 52, issue 10, pp. 6497 - 6507, 2014.

[4] Wilson, T., A. Wu, A. Shrestha, X. Geng, Z. Wang, C. Moeller, R. Frey, and X. Xiong, "Development and Implementation of an Electronic Crosstalk Correction for Bands 27–30 in Terra MODIS Collection 6," Remote Sens., vol. 9, issue 569, 2017.

[5] MODIS Thermal Emissive Band Crosstalk Workshop. MsWG meeting. August 2018. https://mcst.gsfc.nasa.gov/meetings/modis-thermal-emissive-band-crosstalk-workshop.

[6] Chang, T., X. Xiong, A. Shrestha, and C. Perez Diaz, "Methodology development for calibration assessment using quasi-deep convective clouds with application to Aqua MODIS TEB. Earth and Space Science," vol. 7, e2019EA001055, 2020. https://doi.org/10.1029/2019EA001055.

[7] C. Moeller. MODIS and VIIRS TEB Performance. MCST and VCST Calibration Workshop 2019. November 2019.
https://mcst.gsfc.nasa.gov/sites/default/files/meetings_files/03_Moeller_TEBVIIRS.pdf.

[8] Li Y., A. Wu, and X. Xiong, "Assessment of MODIS collection 6.1 thermal emissive band calibration using hyperspectral IASI observations," Proc. SPIE 11530, Sensors, Systems, and Next-Generation Satellites XXIV, 1153019 (20 September 2020); https://doi.org/10.1117/12.2571488.

[9] Chang, T., X. Xiong, and A. Angal, "Terra and Aqua MODIS TEB intercomparison using Himawari-8/AHI as reference", Journal of Applied Remote Sensing, vol. 13, issue 1, pp. 017501, 2019.

[10] Pérez Díaz, C., X. Xiong, and A. Wu, "MODIS thermal emissive bands calibration stability using in-situ ocean targets and remotely-sensed SST retrievals provided by the group for high resolution sea surface temperature," Proc. SPIE 11014, Ocean Sensing and Monitoring XI, 110140P (10 May 2019); https://doi.org/10.1117/12.2518691.

[11] Xiong, X., A. Shrestha, and B. Wenny, "Assessments of MODIS thermal emissive bands on-orbit calibration performance using Dome C observations," Proc. SPIE 10986, Algorithms, Technologies, and Applications for Multispectral and Hyperspectral Imagery XXV, 1098605 (14 May 2019); https://doi.org/10.1117/12.2519000.

[12] Keller, G. R., Z. Wang, A. Wu, and X. Xiong, "Aqua MODIS electronic crosstalk survey from Moon observations," Proc. SPIE 10423, Sensors, Systems, and Next-Generation Satellites XXI, 1042314 (29 September 2017); https://doi.org/10.1117/12.2277972.

[13] Keller, G. R., T. Wilson, X. Geng, A. Wu, Z. Wang and X. Xiong, "Aqua MODIS Electronic Crosstalk Survey: Mid-Wave Infrared Bands," IEEE Transactions on Geoscience and Remote Sensing, vol. 57, no. 3, pp. 1684-1697, 2019, doi: 10.1109/TGRS.2018.2868613.

[14] Chang, T., A. Shrestha, C. Perez Diaz, Y. Li, N. Chen, A. Wu, X. Xiong, "MODIS TEB calibration algorithm improvements for future L1B collection," Proc. SPIE 11501, Earth Observing Systems XXV, 115011H (20 August 2020); https://doi.org/10.1117/12.2567226.